NUCLEAR DEEXCITATION LINES AND UNRESOLVED CONTINUUM IN SOLAR FLARES

R. J. Murphy[1], B. Kozlovsky[2], J. Kiener[3] & G. H. Share[4]

1. Naval Research Laboratory
2. Tel Aviv University
3. Universite Paris-Sud
4. University of Maryland

Overview

- Production of deexcitation gamma-ray lines.
- The gamma-ray line production code and its shortcomings.
- The nuclear reaction code TALYS used to address the shortcomings; its verification and how we use it.
- Examples TALYS calculations.
- How the calculated gamma-ray line spectra obtained with the updated code are used to fit observed solar-flare gamma-ray spectra.

The Variety of Gamma-ray Lines

Nuclear deexcitation lines (0.4 – 7 MeV)

INELASTIC direct

$$\left.\begin{matrix} p \\ \alpha \end{matrix}\right\} + {}^{20}Ne \longrightarrow {}^{20}Ne^{*1.634}$$

INELASTIC inverse

$${}^{20}Ne + \left\{\begin{matrix} H \\ He \end{matrix}\right. \longrightarrow {}^{20}Ne^{*1.634}$$

SPALLATION direct (and inverse)

$$\left.\begin{matrix} p \\ \alpha \end{matrix}\right\} + {}^{24}Mg \longrightarrow {}^{20}Ne^{*1.634} + \ldots$$

FUSION direct (and inverse)

$$\alpha + {}^{24}Mg \longrightarrow {}^{27}Al^{*1.014} + \ldots$$

Neutron-capture line (2.223 MeV)

Positron annihilation line (0.511 MeV)

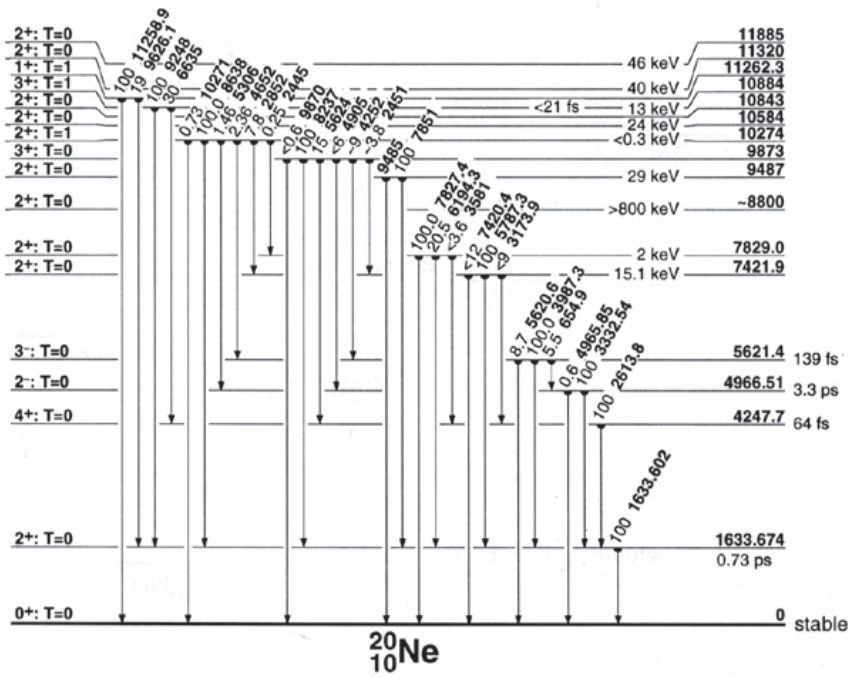

4.438 MeV ^{12}C line
Isotropic accelerated-particle angular distribution

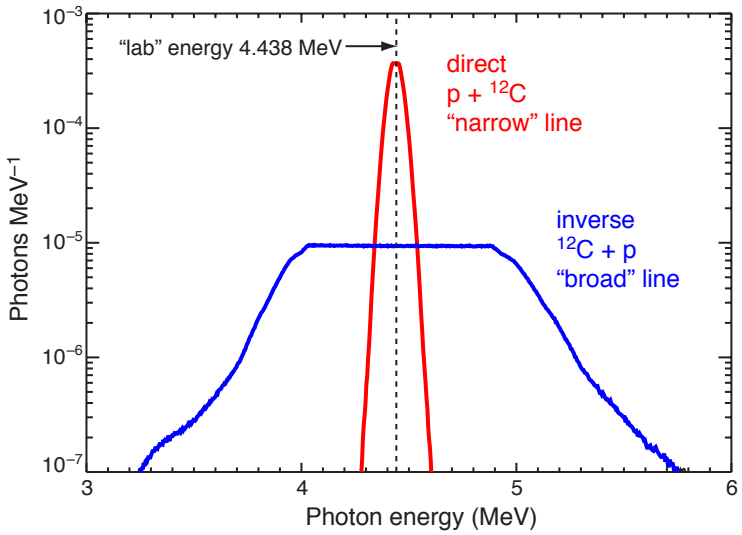

Direct reaction → "narrow" line (FWHM 1 – 2%)

Inverse reaction → "broad" line (FWHM ~20%)

Gamma-Ray Deexcitation-Line Code

Ramaty, Kozlovsky, & Lingenfelter 1979
Kozlovsky, Murphy & Ramaty 2002

Calculates the expected solar-flare deexcitation-line spectrum for a variety of assumed conditions

~100 explicit lines and measured* cross sections

Energy (MeV)	Reaction
0.092	$^{55}Fe^{*1.408} \rightarrow {}^{55}Fe^{*1.317}$
0.110	$^{19}F^{*0.110} \rightarrow$g.s.
0.158	$^{56}Co^{*0.158} \rightarrow$g.s.
0.197	$^{19}F^{*0.197} \rightarrow$g.s.
0.238	$^{19}Ne^{*0.238} \rightarrow$g.s.
0.275	$^{19}Ne^{*0.275} \rightarrow$g.s.
0.339	$^{59}Ni^{*0.339} \rightarrow$g.s.
0.411	$^{55}Fe^{*0.411} \rightarrow$g.s.
0.429	$^{7}Be^{*0.429} \rightarrow$g.s.
0.440	$^{23}Na^{*0.440} \rightarrow$g.s.
0.451	$^{23}Mg^{*0.451} \rightarrow$g.s.
0.477	$^{55}Fe^{*1.408} \rightarrow {}^{55}Fe^{*0.931}$
0.478	$^{7}Li^{*0.478} \rightarrow$g.s.
0.718	$^{10}B^{*0.718} \rightarrow$g.s.
0.744	$^{52}Cr^{*3.114} \rightarrow {}^{52}Cr^{*2.370}$
0.781	$^{27}Si^{*0.781} \rightarrow$g.s.
0.812	$^{56}Co^{*0.970} \rightarrow {}^{56}Co^{*0.158}$
0.835	$^{54}Cr^{*0.835} \rightarrow$g.s.
0.844	$^{27}Al^{*0.844} \rightarrow$g.s.
0.847	$^{56}Fe^{*0.847} \rightarrow$g.s.
0.891	$^{22}Na^{*0.891} \rightarrow$g.s.
0.931	$^{55}Fe^{*0.931} \rightarrow$g.s.
0.936	$^{52}Cr^{*2.370} \rightarrow {}^{52}Cr^{*1.434}$
0.937	$^{18}F^{*0.937} \rightarrow$g.s.
0.957	$^{27}Si^{*0.957} \rightarrow$g.s.
0.984	$^{48}Ti^{*0.984} \rightarrow$g.s.
0.999	$^{59}Ni^{*1.338} \rightarrow {}^{59}Ni^{*0.339}$
1.005	$^{58}Ni^{*2.459} \rightarrow {}^{58}Ni^{*1.454}$
1.014	$^{27}Al^{*1.014} \rightarrow$g.s.
1.022	$^{10}B^{*1.740} \rightarrow {}^{10}B^{*0.718}$
1.038	$^{56}Fe^{*3.123} \rightarrow {}^{56}Fe^{*2.085}$
1.042	$^{18}F^{*1.042} \rightarrow$g.s.
1.049	$^{58}Co^{*1.049} \rightarrow$g.s.
1.081	$^{18}F^{*1.081} \rightarrow$g.s.
1.130	$^{54}Fe^{*2.538} \rightarrow {}^{54}Fe^{*1.408}$

Energy (MeV)	Reaction
1.189	$^{59}Ni^{*1.189} \rightarrow$g.s.
1.190	$^{59}Co^{*1.190} \rightarrow$g.s.
1.223	$^{55}Fe^{*2.539} \rightarrow {}^{55}Fe^{*1.317}$
1.238	$^{56}Fe^{*2.085} \rightarrow {}^{56}Fe^{*0.847}$
1.249	$^{31}S^{*1.249} \rightarrow$g.s.
1.266	$^{31}P^{*1.266} \rightarrow$g.s.
1.275	$^{22}Ne^{*1.275} \rightarrow$g.s.
1.312	$^{48}Ti^{*2.296} \rightarrow {}^{48}Ti^{*0.984}$
1.317	$^{55}Fe^{*1.317} \rightarrow$g.s.
1.334	$^{52}Cr^{*2.768} \rightarrow {}^{52}Cr^{*1.434}$
1.367	$^{59}Ni^{*2.705} \rightarrow {}^{59}Ni^{*1.338}$
1.369	$^{24}Mg^{*1.369} \rightarrow$g.s.
1.370	$^{55}Fe^{*2.301} \rightarrow {}^{55}Fe^{*0.931}$
1.408	$^{55}Fe^{*1.408} \rightarrow$g.s.
1.428	$^{59}Ni^{*1.767} \rightarrow {}^{59}Ni^{*0.339}$
1.434	$^{52}Cr^{*1.434} \rightarrow$g.s.
1.441	$^{53}Mn^{*1.441} \rightarrow$g.s.
1.454	$^{58}Ni^{*1.454} \rightarrow$g.s.
1.460	$^{59}Co^{*1.460} \rightarrow$g.s.
1.600	$^{23}Mg^{*2.051} \rightarrow {}^{23}Mg^{*0.451}$
1.635	$^{14}N^{*3.948} \rightarrow {}^{14}N^{*2.313}$
1.634	$^{20}Ne^{*1.634} \rightarrow$g.s.
1.636	$^{23}Na^{*2.076} \rightarrow {}^{23}Na^{*0.440}$
1.771	$^{56}Fe^{*3.856} \rightarrow {}^{56}Fe^{*2.085}$
1.779	$^{28}Si^{*1.779} \rightarrow$g.s.
1.809	$^{26}Mg^{*1.809} \rightarrow$g.s.
1.811	$^{56}Fe^{*2.658} \rightarrow {}^{56}Fe^{*0.847}$
2.000	$^{11}C^{*2.000} \rightarrow$g.s.
2.029	$^{31}P^{*3.295} \rightarrow {}^{31}P^{*1.266}$
2.034	$^{31}S^{*3.283} \rightarrow {}^{31}S^{*1.249}$
2.094	$^{56}Fe^{*2.942} \rightarrow {}^{56}Fe^{*0.847}$
2.113	$^{56}Fe^{*2.960} \rightarrow {}^{56}Fe^{*0.847}$
2.124	$^{11}B^{*2.125} \rightarrow$g.s.
2.164	$^{27}Si^{*2.164} \rightarrow$g.s.
2.211	$^{27}Al^{*2.211} \rightarrow$g.s.

Energy (MeV)	Reaction
2.230	$^{32}S^{*2.230} \rightarrow$g.s.
2.232	$^{31}S^{*2.232} \rightarrow$g.s.
2.234	$^{31}P^{*2.234} \rightarrow$g.s.
2.263	$^{23}Na^{*2.704} \rightarrow {}^{23}Na^{*0.440}$
2.313	$^{14}N^{*2.313} \rightarrow$g.s.
2.598	$^{56}Fe^{*3.449} \rightarrow {}^{56}Fe^{*0.847}$
2.614	$^{20}Ne^{*4.248} \rightarrow {}^{20}Ne^{*1.634}$
2.640	$^{23}Na^{*2.640} \rightarrow$g.s.
2.742	$^{16}O^{*8.872} \rightarrow {}^{16}O^{*6.130}$
2.754	$^{24}Mg^{*4.123} \rightarrow {}^{24}Mg^{*1.369}$
3.333	$^{20}Ne^{*4.967} \rightarrow {}^{20}Ne^{*1.634}$
3.562	$^{6}Li^{*3.563} \rightarrow$g.s.
3.684	$^{13}C^{*3.685} \rightarrow$g.s.
3.736	$^{40}Ca^{*3.736} \rightarrow$g.s.
3.853	$^{13}C^{*3.854} \rightarrow$g.s.
4.438	$^{12}C^{*4.439} \rightarrow$g.s.
4.444	$^{11}B^{*4.445} \rightarrow$g.s.
5.099	$^{28}Si^{*6.879} \rightarrow {}^{28}Si^{*1.779}$
5.105	$^{14}N^{*5.106} \rightarrow$g.s.
5.180	$^{15}O^{5.181} \rightarrow$g.s.
5.240	$^{15}O^{*5.241} \rightarrow$g.s.
5.269	$^{15}N^{*5.270} \rightarrow$g.s.
5.298	$^{15}N^{*5.299} \rightarrow$g.s.
6.129	$^{16}O^{*6.130} \rightarrow$g.s.
6.175	$^{15}O^{*6.176} \rightarrow$g.s.
6.322	$^{15}N^{*6.324} \rightarrow$g.s.
6.337	$^{11}C^{*6.339} \rightarrow$g.s.
6.476	$^{11}C^{*6.478} \rightarrow$g.s.
6.741	$^{11}B^{*6.743} \rightarrow$g.s.
6.790	$^{11}B^{*6.792} \rightarrow$g.s.
6.879	$^{28}Si^{*6.879} \rightarrow$g.s.
6.916	$^{16}O^{*6.917} \rightarrow$g.s.
7.115	$^{16}O^{*7.117} \rightarrow$g.s.
7.299	$^{15}N^{*7.301} \rightarrow$g.s.
15.10	$^{12}C^{*15.11} \rightarrow$g.s.

***varying degrees of completeness**

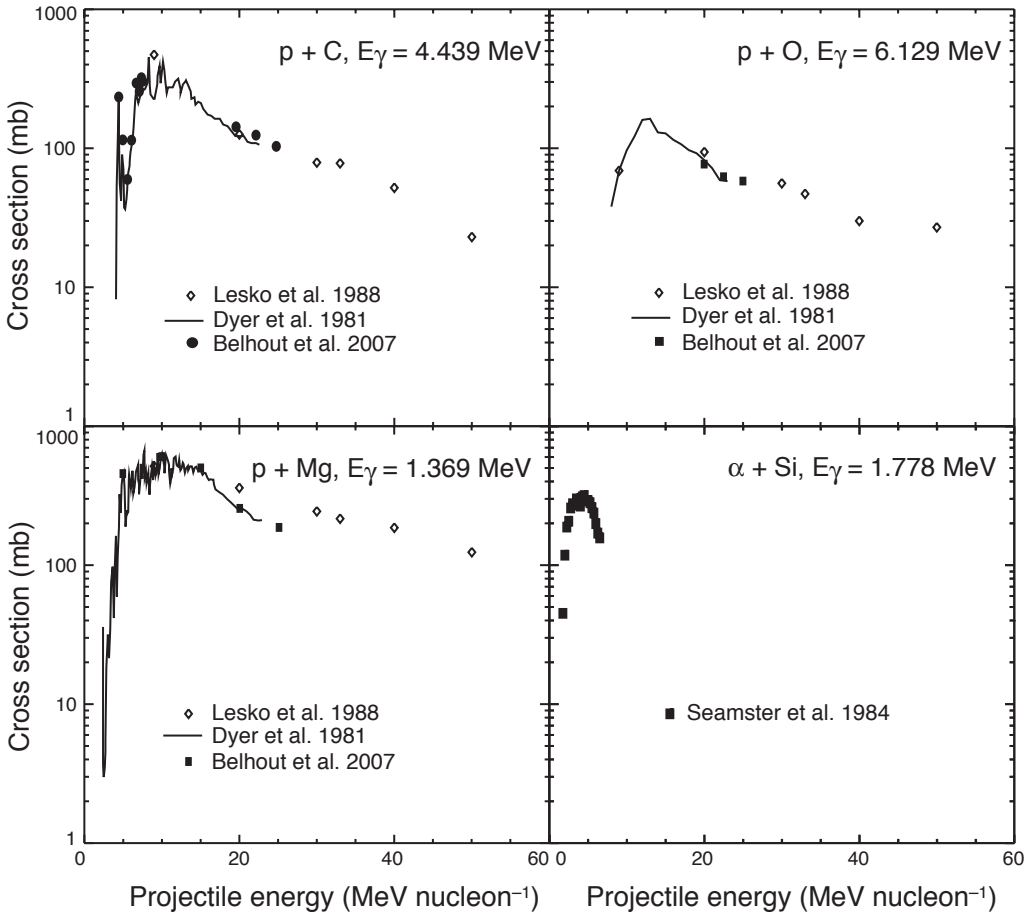

Unresolved Gamma-Ray Line Continuum

But the bulk of emission from energetic-ion interactions with ambient material arises from numerous, relatively weak lines, especially from nuclei heavier than oxygen.

For very heavy nuclei, such as iron, the number of lines can number in the hundreds, and the number of product nuclei via spallation or fusion can be very numerous, espicially for higher-energy reactions.

The total number of lines can be so numerous and closely-spaced that they merge into a quasi-continuum, called the "unresolved-line continuum".

In the RKL gamma-ray line code, this component was estimated from low spectral-resolution laboratory measurements of the total gamma-ray spectrum for only a few target nuclei and at only a few projectile energies. In the code, only proton interactions with Ne, Mg, Si and Fe were included, and the spectra were assumed to be independent of projectile energy.

TALYS

To provide this information about the unresolved-line continuum, we have used the global-nuclear theoretical program TALYS. (Koning, Hilaire & Duijvestijn 2005; Koning & Duijvestijn 2006)

TALYS is software for the simulation of nuclear reactions using state-of-the-art nuclear models and comprehensive libraries of nuclear data, developed at NRG Petten, the Netherlands and CEA Bruyeres-le-Chatel, France.

TALYS attempts to provide a complete and accurate simulation of nuclear reactions in the 1 keV-200 MeV energy range, through an optimal combination of reliable nuclear models, flexibility and user-friendliness.

TALYS will also allow us to check our assumptions about those explicit line cross sections in our code for which complete measurements are not available and to include lines for which no measurements are available.

TALYS

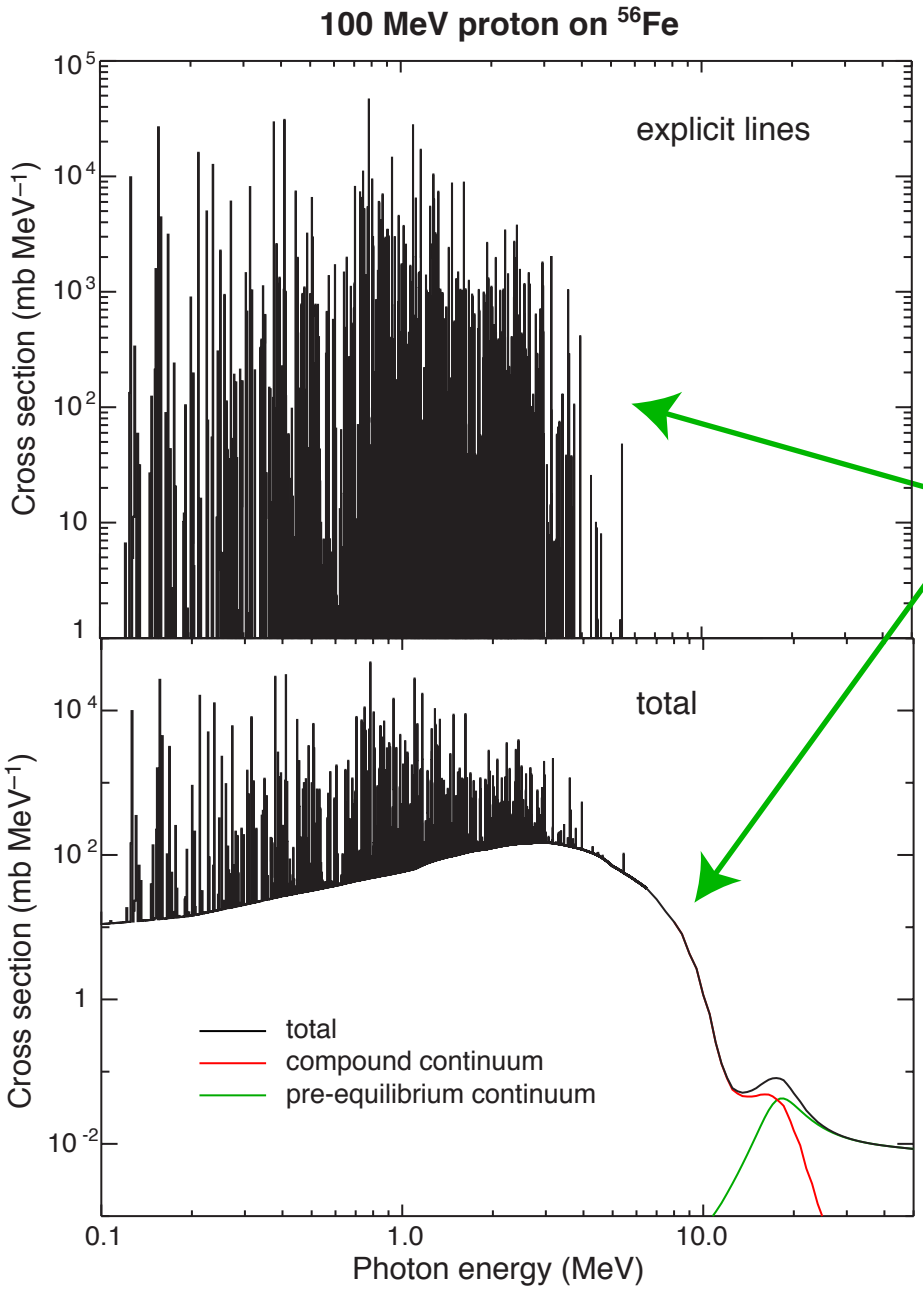

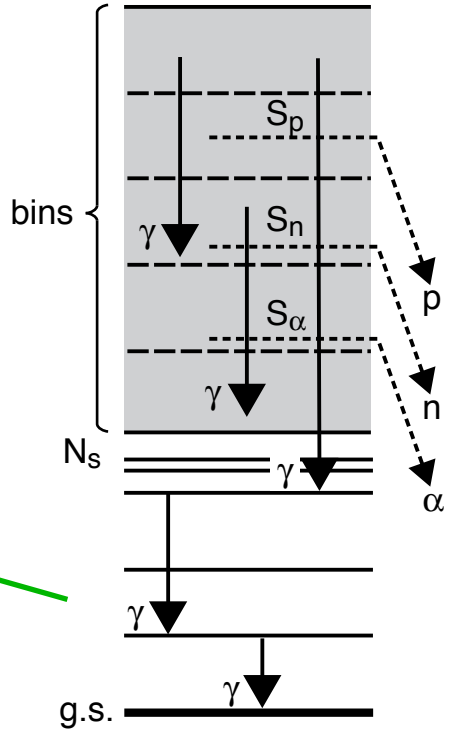

TALYS treats low-lying transitions explicitly and higher-lying transitions as a continuous spectrum

Note appearance of structure due to clusters of lines

VERIFICATION OF TALYS

The TALYS authors have verifed its accuracy by comparing calculated results for a variety of nuclear reactions with experimental data. The demonstrated success of TALYS is remarkable, but most of these tests and comparisons dealt with particle-emitting reactions on very heavy targets.

We have therefore extended the testing of TALYS to those gamma-ray producing reactions where experimental data are available.

CONFIRMATION OF TALYS ACCURACY

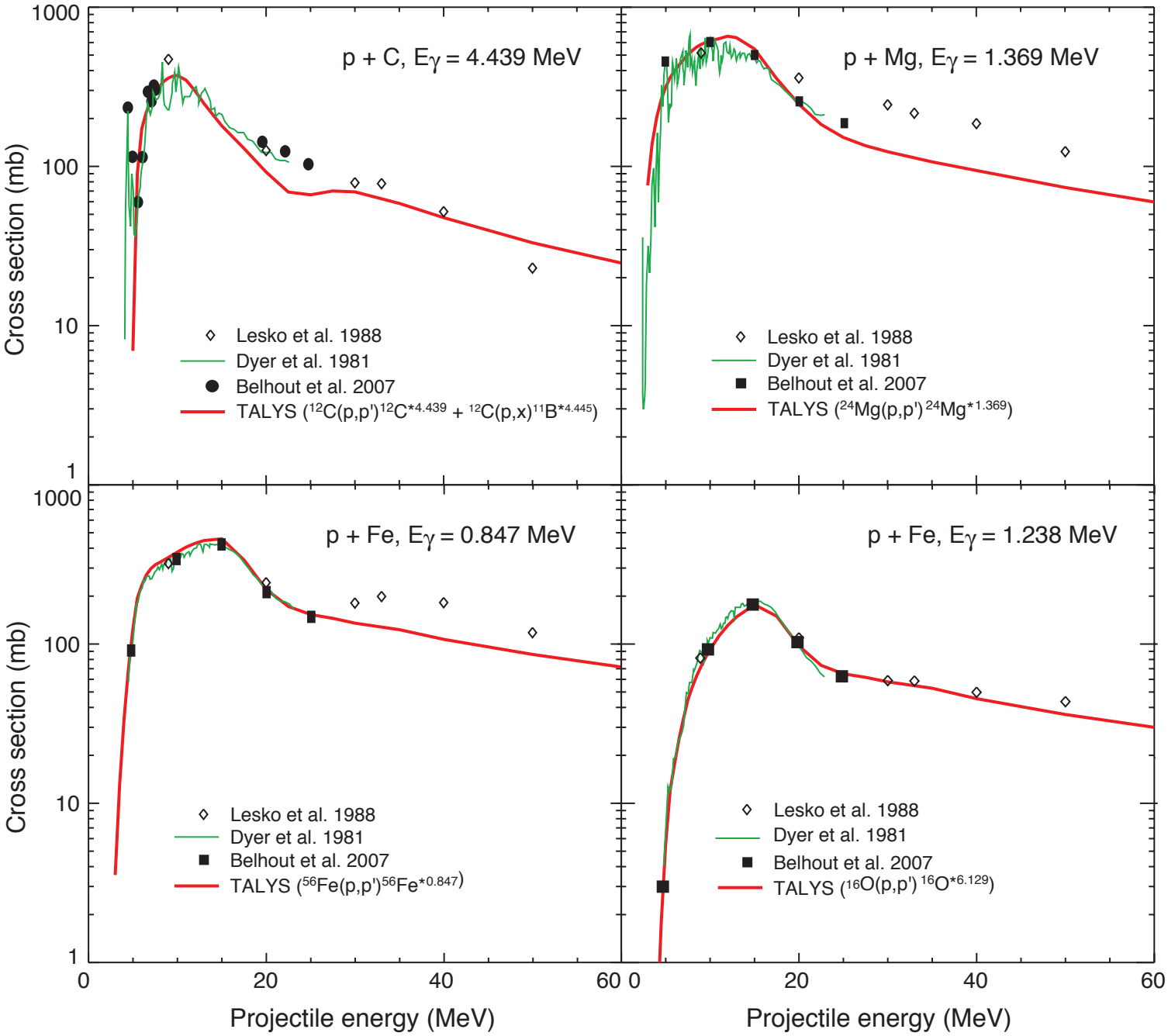

Improved Explicit Deexcitation-Line Cross Sections

We have used TALYS to provide cross sections for intermediate-strength lines with no measured cross sections. There now are 250 explicit lines in the code.

TALYS has also improved many "measured" cross sections.

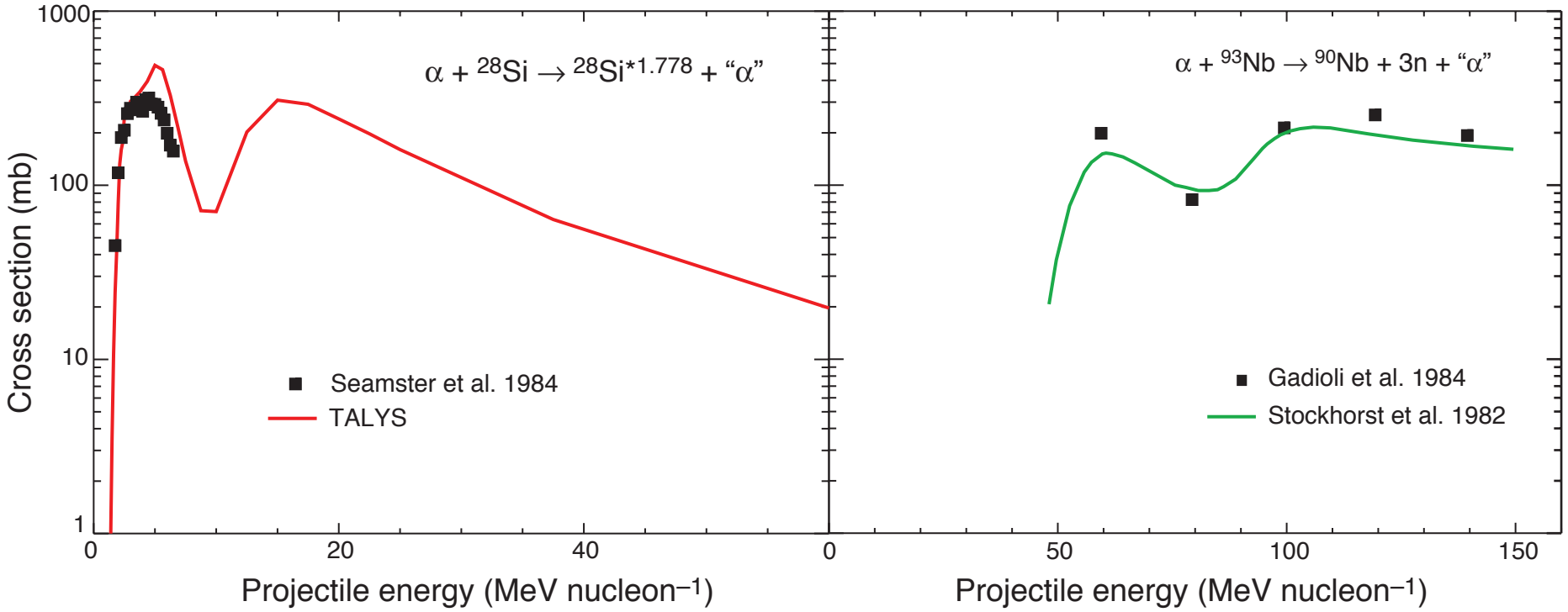

TOTAL UNRESOLVED-LINE CROSS SECTIONS

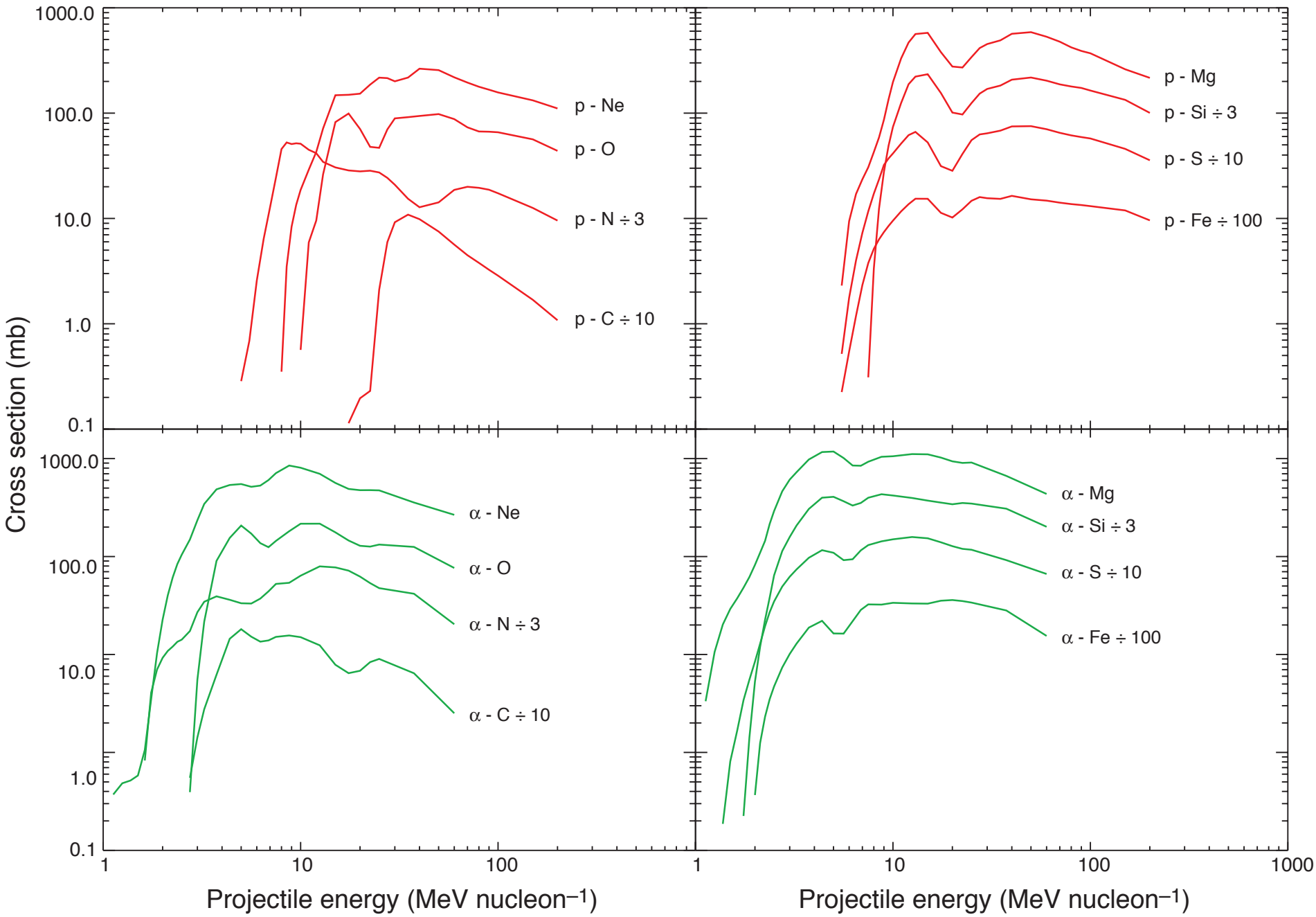

DEPENDENCE OF UNRESOLVED-LINE CONTINUUM ON PROJECTILE ENERGY

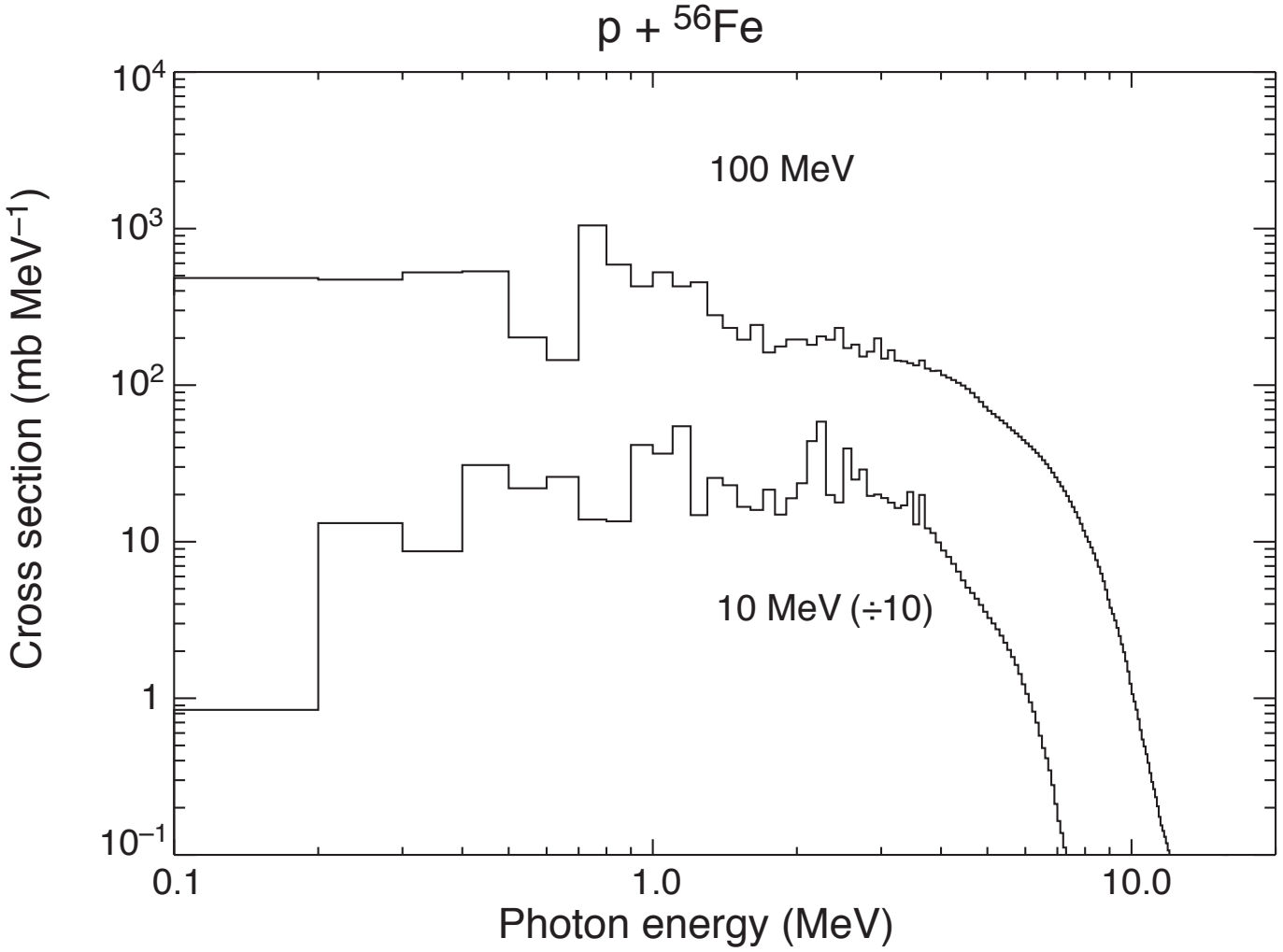

Note: the spectra have been rebinned into 100-keV bins.

DEPENDENCE OF UNRESOLVED-LINE CONTIUNUUM ON TARGET SPECIES

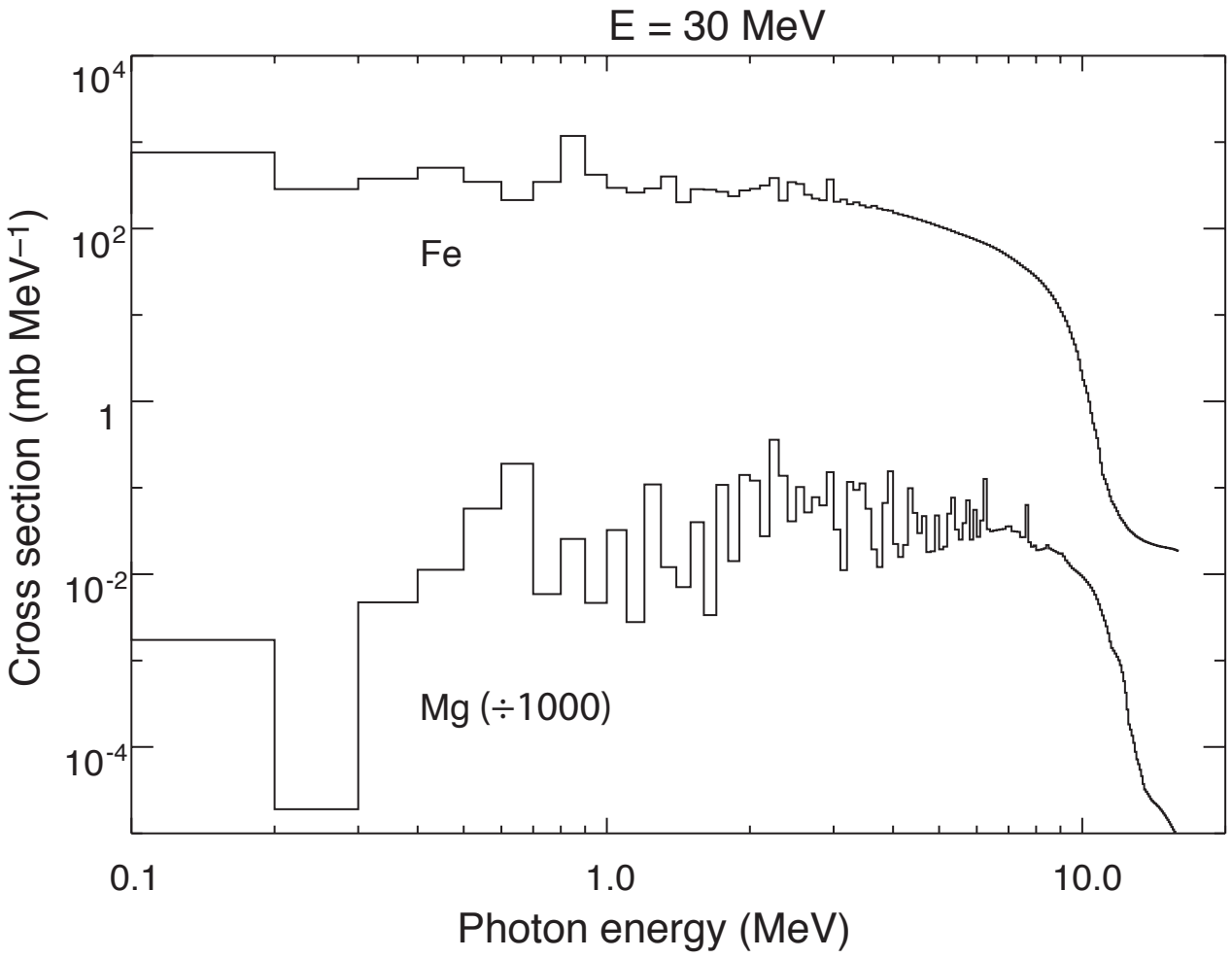

The total gamma-ray deexcitation-line spectrum depends on:

1. acccelerated-ion energy spectrum

2. acccelerated-ion angular distribution

3. ambient abundances

4. accelerated-ion abundances

TOTAL GAMMA-RAY DEEXCITATION-LINE SPECTRUM

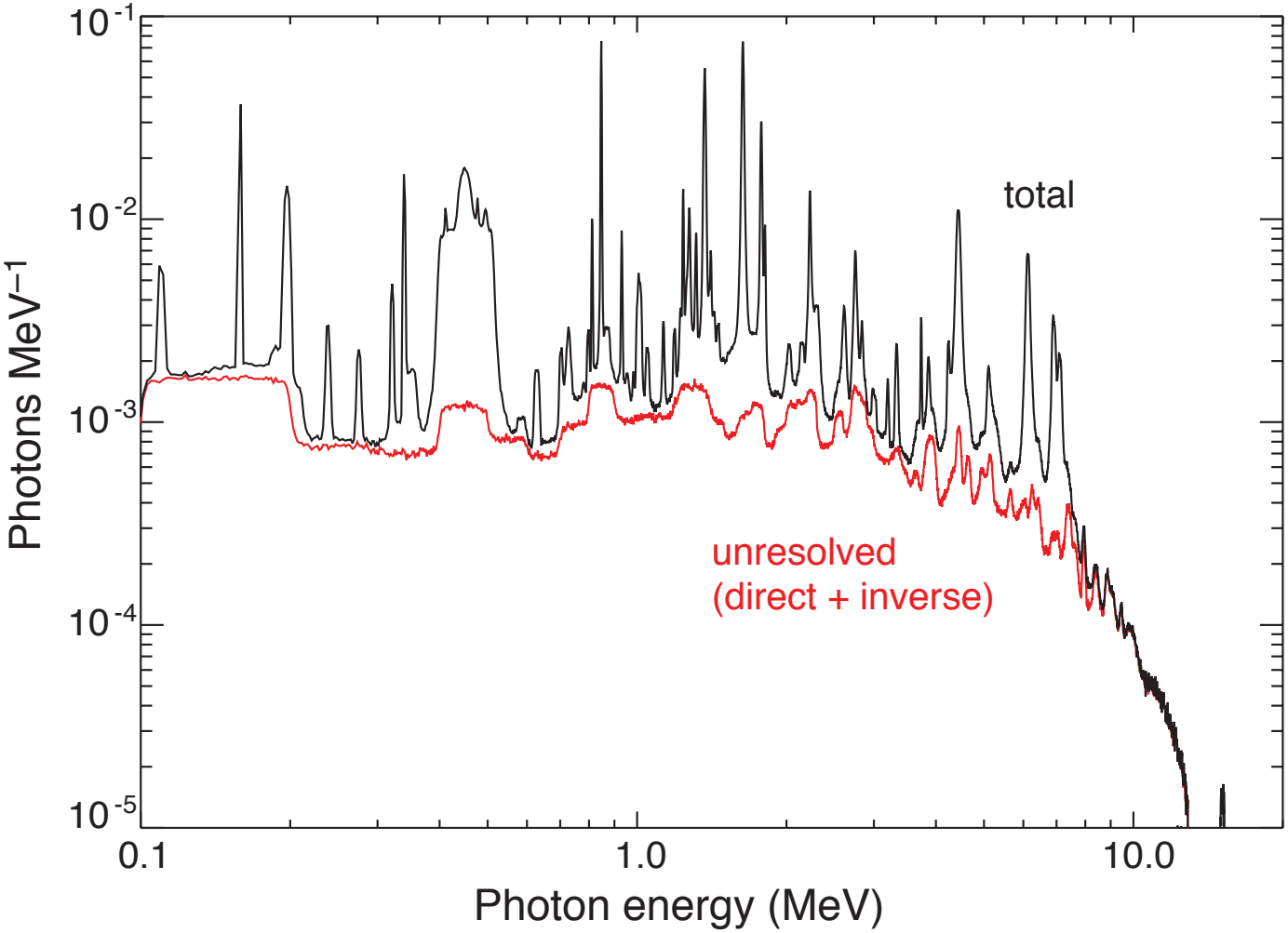

acccelerated-ion spectral index = 4.0

isotropic angular distribution

coronal ambient abundances (but He/H = 0.1)

coronal accelerated-ion abundances (but α/proton = 0.1)

USE FOR FITTING OBSERVED SOLAR-FLARE GAMMA-RAY SPECTRA

For assumed:

1. accelerated-ion spectral index s
2. accelerated-ion alpha/proton ratio α/p
3. accelerated-ion angular distribution

calculate the 16 elemental ambient and accelerated-ion spectra:

1. p + α on 8 ambient elements (^{4}He, C, N, O, Ne, Mg, Si, Fe)
2. 8 accelerated-ions (^{3}He, C, N, O, Ne, Mg, Si, Fe) on ambient H + He

Do this for a grid of indexes and alpha/proton ratios.

For each combination of s and α/p, find the linear combination of the 16 spectra that best fits an observed spectrum. The fitted relative amplitudes represent the relative abundances.

The best fit provides the spectral index and alpha/proton ratio.

ELEMENTAL SPECTRA FOR AMBIENT MATERIAL

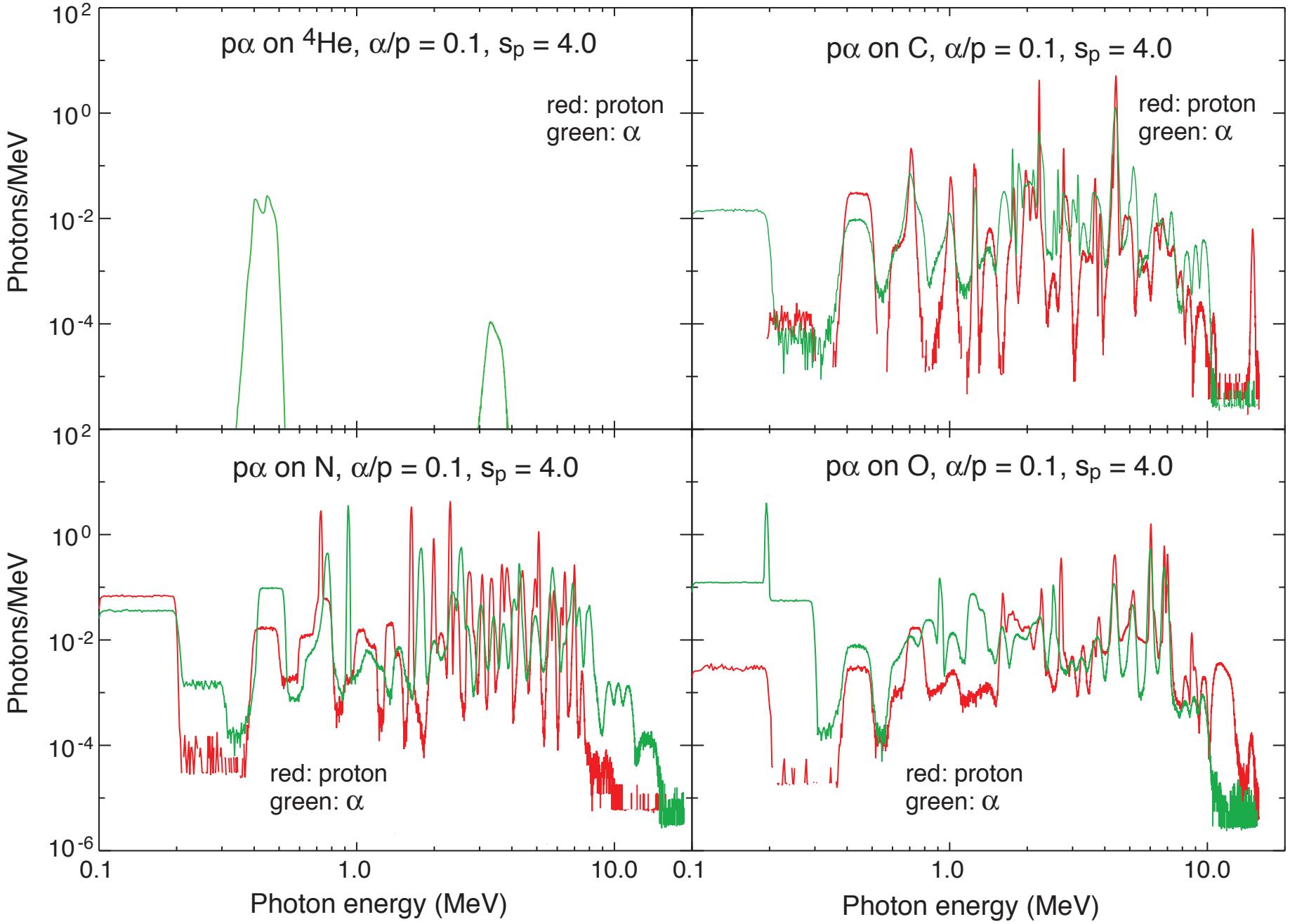

ELEMENTAL SPECTRA FOR AMBIENT MATERIAL

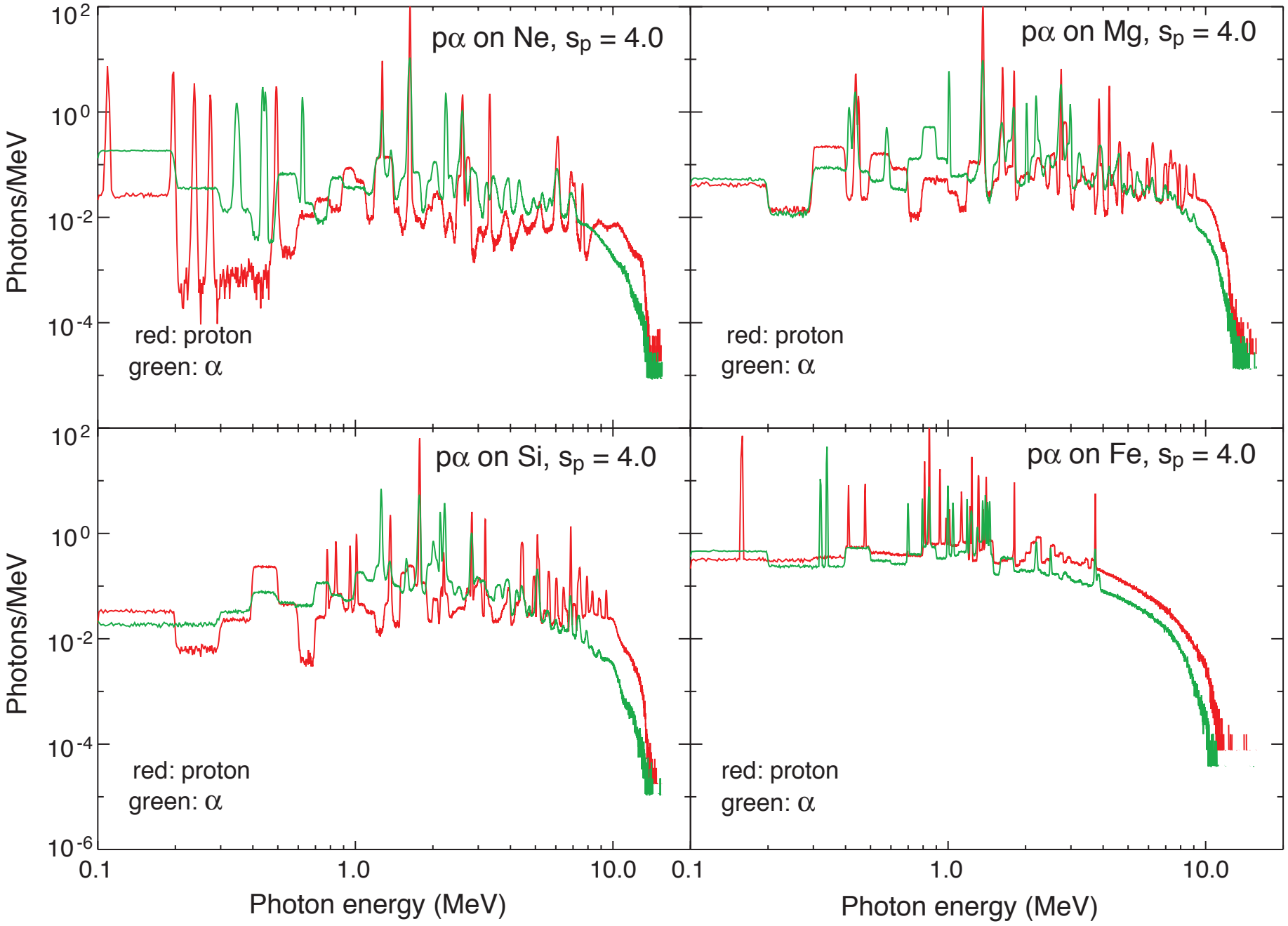

ELEMENTAL SPECTRA FOR ACCELERATED IONS

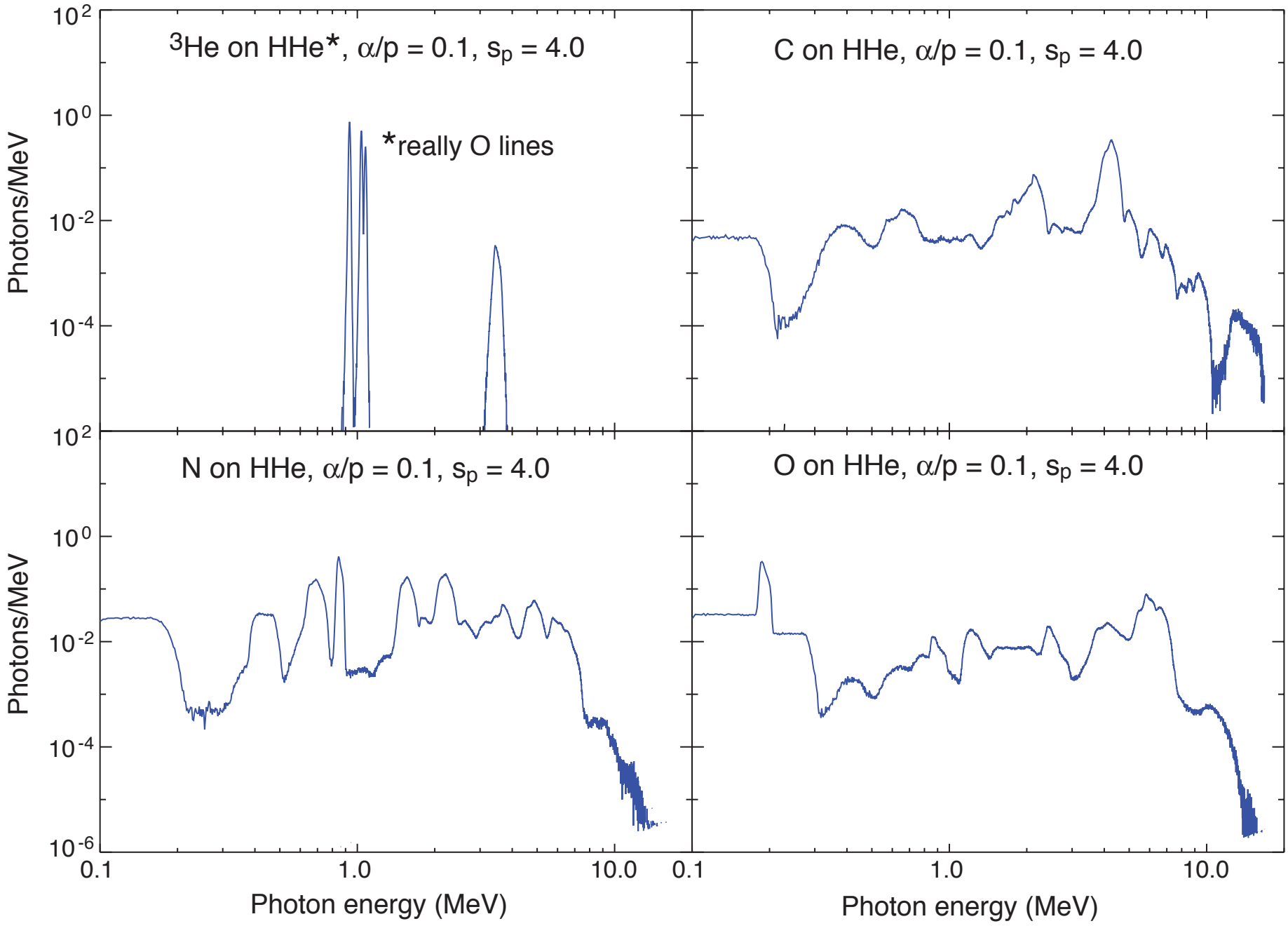

ELEMENTAL SPECTRA FOR ACCELERATED IONS